Further Results on Detection and Channel Estimation for Hardware Impaired Signals

Yunfei Chen, *Senior Member, IEEE*, Zhutian Yang, Jie Zhang, Mohamed-Slim Alouini, *Fellow, IEEE*

***Abstract*— Hardware impairment is inevitable in many wireless systems. It is particularly severe in low-cost applications due to the imperfect components used. In this paper, the channel estimation and non-coherent detection problems of hardware impaired signals are studied for a single-carrier, single-antenna and single-hop system. Specifically, three different cases are investigated: signals with additive distortion only, signals with in-phase and quadrature imbalance only, and signals with both impairments. The maximum likelihood and Gaussian approximation methods are used to derive the new non-coherent detectors for amplitude modulated signals, while the maximum likelihood and moment-based methods are employed to design the new channel estimators for all signals. Numerical results show that the new non-coherent detectors outperform the existing non-coherent detectors in the presence of hardware impairment. The performance gain can be as high as 8 dB. They also show that the new channel estimators have much higher accuracy than the existing estimator. In some conditions, the accuracy of the new estimator is about 100 times that of the existing estimator.**

***Index Terms*— Channel estimation, hardware impairment, non-coherent detection.**

I. Introduction

Wireless communication has seen unprecedented development in recent years. To enable such a development, the use of low-cost wireless devices is crucial. Due to this, it is inevitable that the quality of the components used in these devices may not meet a high standard, leading to hardware impairment (HWI).

There have been considerable amount of research work conducted on HWI in wireless systems. To name a few, in [2], the effect of in-phase and quadrature imbalance (IQI) on the outage probability and symbol error rate of a single-antenna multi-carrier system was discussed. This was further extended to multiple-input-multiple-output (MIMO) systems in [3] and [4] and relaying systems in [5] - [8]. In [9], the effect of additive distortion (AD) due to phase noise and nonlinear power amplification on the outage performance of a receiver diversity system was examined. More works have been conducted on relaying systems. For example, in [10] and [11], the effect of AD on the performances of two-way relaying systems was studied. Similar studies were also performed for one-way relaying using amplify-and-forward or decode-and-forward protocols. Reference [12] evaluated the effect of AD in a non-orthogonal multiple access system, [13] considered it in a full-duplex massive MIMO system, [14] studied it for a mixture of radio and optical links, [15] applied it to the beamforming design of a MIMO system, while [16] - [18] examined it in a hybrid satellite and terrestrial network with a mixture of satellite and terrestrial links. On the other hand, references [19] and [20] investigated a generic relaying system. Moreover, the effect of AD in the presence of other imperfection, such as channel estimation errors, was also studied in [21] - [24] (Due to the limited space, we only mention four of them here). Similar to [12], [25] and [26] also derived the performance of non-orthogonal multiple access system with IQI or phase noise, but without relaying.

The aforementioned works consider either IQI or AD but not both. There have been very few works that consider both HWIs. For example, in [27], energy detection with both IQI and AD was examined. The model used in [27] distinguishes AD by phase noise from that by amplification and only studies distortions at the receiver. Reference [28] looked into the effects of both IQI and AD on the performance of a single antenna single-hop system, [29] studied them for a multi-antenna and single-hop system, while [30] discussed a single-antenna dual-hop system with HWI at source, relay as well as destination.

The above works have mainly evaluated the effect of HWI on the wireless performances. However, when the HWI is present, it may be necessary to re-design the wireless system for the best performance, as knowledge of the HWI can be utilized in the design to improve system performance. In this regard, reference [31] proposed a new optimal detector for spatial modulation in the presence of IQI. A similar detector was also proposed for amplify-and-forward relaying by the same authors [32]. Reference [33] derived a new detector for teraHertz systems considering nonlinear power amplification at the transmitter, while reference [28] designed a new optimal detector in the presence of both IQI and AD. Similarly, references [36] and [37] studied the use of linear minimum mean squared error (LMMSE) and deep learning in the channel estimation of massive MIMO systems with nonlinear amplification using deterministic behavioral models, references [38] and [39] applied sparse recovery and expectation-maximization to estimate massive MIMO channels with nonlinear amplification using stochastic models, while references [40] and [41] used

The work of Yunfei Chen is supported in part by EC H2020 DAWN4IoE-Data Aware Wireless Network for Internet-of-Everything under Grant 778305. The corresponding author is Zhutian Yang.

Yunfei Chen is with the School of Engineering, University of Warwick, Coventry, CV4 7AL, UK (e-mail: Yunfei.Chen@warwick.ac.uk).

Zhutian Yang is with the School of Electronics and Information Engineering, Harbin Institute of Technology, Harbin, China, 150001. (e-mail: yangzhutian@hit.edu.cn)

J. Zhang is with the Department of Electronic and Electrical Engineering, Sheffield University, Sheffield, S1 4DE, UK (e-mail: jie.zhang@sheffield.ac.uk).

Mohamed-Slim Alouini is with the EE program, King Abdullah University of Science and Technology, Thuwal, Mekkah Province, Saudi Arabia (e-mail: slim.alouini@kaust.edu.sa).

LMMSE for massive MIMO channels with IQI.

All the above works have provided very useful guidance and insights on the designs of wireless systems suffering from HWI. However, two further studies are still necessary. Firstly, most existing channel estimators have only considered AD or IQI but not both. Also, the existing estimators are very complicated. Secondly, to further reduce the cost of device, non-coherent detection can be employed, as it does not require channel estimators, at the cost of performance loss compared with coherent detection. Most existing works have not investigated the problem of non-coherent detection for hardware impaired signals. References [34] and [35] evaluated the performances of existing non-coherent detectors subject to HWI but did not derive any new non-coherent detectors.

Motivated by the above observations, in this paper, the problems of channel estimation and non-coherent detection using hardware impaired wireless signals are studied for a single-antenna, single-carrier and single-hop wireless system. Three different cases are considered: the signals suffer from AD only, the signals suffer from IQI only, and the signals suffer from both AD and IQI. Approximate maximum likelihood (ML) and Gaussian approximation methods are used to derive the new non-coherent detectors for amplitude modulation. For channel estimation, new estimators are developed by using both ML and moment-based (MB) methods for any modulation. The performances of the new estimators are examined in terms of the mean squared error (MSE) as well as the error rates of coherent detectors employing them. Numerical results show that the new non-coherent detectors have significant performance gains over the existing non-coherent detector, especially when the signal-to-noise ratio (SNR) is large. Also, the new channel estimators outperform the conventional ML estimators that ignore HWI in most cases. Under some reasonable conditions, the accuracy of the new estimator is 100 times that of the existing estimator. The novelty and the contribution of this work are summarized as follows.

- New non-coherent detectors for hardware impaired signals are derived. Compared with the previous works in [2] - [33], the new non-coherent detectors do not require channel state information to reduce cost. Also, compared with conventional non-coherent detectors, the new detectors take HWI models into account to improve detection performance. This improvement could be as large as 8 dB in SNR in some cases.
- New channel estimators for hardware impaired signals are derived. Compared with [36] - [41], our estimators are much simpler and consider both AD and IQI. Also, compared with the conventional ML channel estimator ignoring HWI, our new estimators improves the accuracy. The MSE of the new estimator could be 100 times smaller than the conventional ML estimator ignoring HWI.
- In addition to the derivations of new detectors and estimators, this work thoroughly investigates the performances of HWI signal detectors and estimators by considering and quantifying the effects of important parameters.

The rest of the paper is organized as follows. In Section II, the system model will be discussed. In Section III, new non-coherent detectors for hardware impaired signals will be proposed. Section IV gives the newly designed channel estimators for hardware impaired signals. Section V presents the numerical examples to show the advantages and disadvantages of the new detectors and estimators. Finally, concluding remarks are made in Section VI.

Notations: In the following, unless otherwise specified, $E\{\cdot\}$ represents the expectation operation, $\mathcal{CN}(\cdot,\cdot)$ represents a complex Gaussian random variable, $(\cdot)^*$ represents the conjugate operation, $\arg_x$ denotes the value of x satisfying certain criterion, $\min\{\cdot\}$ denotes the minimum, $\ln$ denotes the natural logarithm, $\sin(\cdot)$ denotes the sine function.

II. System Model

Consider a wireless communications system where both transmitter and receiver have one single antenna. Assume that the transmitted information signal is x with $E\{|x|^2\} = P$. When there is no HWI, the received signal is given by

$$y = hx + n, \tag{1}$$

where h is the fading channel gain following a complex Gaussian distribution with $h \sim \mathcal{CN}(0, \sigma_h^2)$ so that the Rayleigh fading model is assumed, and n is the additive white Gaussian noise (AWGN) with $n \sim \mathcal{CN}(0, \sigma_n^2)$. Assume that h, x and n are independent. When HWI occurs, three different cases will be discussed in the following.

A. AD Only

In the first case when there is only AD caused by power amplifiers, the received signal is given as [1]

$$y = h(x + d) + n, \tag{2}$$

where d represents the AD caused by imperfect power amplification and follows a complex Gaussian distribution with $d \sim \mathcal{CN}(0, (\sigma_t^2 + \sigma_r^2)P)$, σ_t^2 is the variance of the AD at the transmitter, σ_r^2 is the variance of the AD at the receiver, and P, x, h and n are defined as before. The parameters of σ_t^2 and σ_r^2 come from numerous theoretical analysis and measurement results. It is also motivated by the central limit theorem to model the aggregate distortion from various RF stages. Assume that d is independent of h and n. The model in (2) has been widely used in the literature, such as [9] - [30]. Detailed explanation can be found in [1]. Define $\epsilon = \frac{\sigma_h^2}{(\sigma_t^2+\sigma_r^2)P}$ as the signal-to-distortion ratio (SDR). The SDR increases when the distortion decreases.

B. IQI Only

In the second case when there is only IQI caused by imperfect phase shifter or mismatched local oscillator, the received signal is given as [28]

$$y = K_1(hx_q + n) + K_2(hx_q + n)^*, \tag{3}$$

where $x_q = G_1 x + G_2^* x^*$ is a widely linear transformed signal of the transmitted information signal x due to the IQI at the transmitter, $G_1 = \frac{1}{2}(1 + \zeta_T e^{j\phi_T})$ and $G_2 = \frac{1}{2}(1 - \zeta_T e^{-j\phi_T})$ are the IQI coefficients at the transmitter, ζ_T represents the

amplitude mismatch at the transmitter, ϕ_T represents the phase mismatch at the transmitter, $K_1 = \frac{1}{2}(1 + \zeta_R e^{j\phi_R})$ and $K_2 = \frac{1}{2}(1 - \zeta_R e^{-j\phi_R})$ are the IQI coefficients at the receiver from [28], ζ_R represents the amplitude mismatch at the receiver, ϕ_R represents the phase mismatch at the receiver, h and n are the fading channel gain and the AWGN, respectively, as defined before. Note that we follow the model in [28] for K_1 and K_2, while other works, such as [1], use $K_1 = \frac{1}{2}(1+\zeta_R e^{-j\phi_R})$ and $K_2 = \frac{1}{2}(1 - \zeta_R e^{j\phi_R})$. Their only difference is the polarity of the phase. Thus, one can easily obtain results for the model in [1] by replacing ϕ_R with $-\phi_R$ in the following. The parameters of ζ_T, ζ_R, ϕ_T and ϕ_R come from the amplitude and phase mismatch between the in-phase and quadrature branches of the local oscillator, as $a_Q(t) = \zeta_T \sin(\omega_c t + \phi_T)$ and $a_I(t) = \cos(\omega_c t)$ at transmitter before up-conversion and $b_Q(t) = -\zeta_R \sin(\omega_c t - \phi_R)$ and $b_I(t) = \cos(\omega_c t)$ at receiver before down-conversion, where ω_c is the carrier frequency. Substituting the expression of x_q into (3), one further has

$$y = gx + fx^* + z, \tag{4}$$

where

$$g = K_1 G_1 h + K_2 G_2 h^*, \tag{5a}$$

$$f = K_1 G_2^* h + K_2 G_1^* h^*, \tag{5b}$$

$$z = K_1 n + K_2 n^*. \tag{5c}$$

In this case, $gx + fx^*$ is the signal component in the received signal and z is the noise component in the received signal. This model has also been widely used in the IQI literature, such as [2] - [8]. Compared with the conventional model in (1), the IQI leads to extra terms in the signal component containing x^* and h^* as well as extra term in the noise component containing n^*. This makes the signal and noise improper Gaussian [42]. The image rejection ratio is defined as $\frac{|G_1|^2}{|G_2|^2}$ at transmitter and $\frac{|K_1|^2}{|K_2|^2}$ at receiver that quantifies the level of IQI. When $\phi_T = 0$, $\zeta_T = 1$ or $\phi_R = 0$, $\zeta_R = 1$, there is no IQI at the transmitter or receiver, respectively. If both $\phi_T = 0$, $\zeta_T = 1$ and $\phi_R = 0$, $\zeta_R = 1$, the hardware becomes perfect.

C. AD and IQI

In the third case, the system suffers from both AD caused by nonlinear power amplification and IQI caused by phase and amplitude mismatch. Then, the received signal is given by

$$y = K_1 y_q + K_2 y_q^*, \tag{6}$$

where

$$y_q = h(x_q + e) + n, \tag{7}$$

and all the parameters are defined as before except the AD e now follows a complex Gaussian distribution with $e \sim \mathcal{CN}(0, (\sigma_t^2 + \sigma_r^2)P')$ and $P' = E\{|x_q|^2\} = E\{|G_1 x + G_2 x^*|^2\}$. Substituting (7) and the expression of x_q into (6), one further has

$$y = gx + fx^* + w, \tag{8}$$

where

$$w = K_1 n + K_2 n^* + K_1 e h + K_2 e^* h^*, \tag{9}$$

and g, f are defined in (5). It is easy to see that (2) and (4) are special cases of (6) when there is no IQI or AD, respectively. Also, in the following, parameters of AD and IQI are required. These parameters could change with temperature etc. However, these changes are slow compared with fading and therefore, their values can be obtained before detection and estimation, as in [2] - [41]. For later use, the improper Gaussian probability density function (PDF) is given as follows.

Preliminary: The improper Gaussian PDF is defined as

$$f(x) = \frac{e^{-\frac{1}{2(1-\rho^2)}\left[\frac{(x_R - m_R)^2}{\sigma_R^2} + \frac{(x_I - m_I)^2}{\sigma_I^2} - \frac{2\rho(x_R - m_R)(x_I - m_I)}{\sigma_R \sigma_I}\right]}}{2\pi\sigma_R\sigma_I\sqrt{1-\rho^2}} \tag{10}$$

where x_R is the real part of x, x_I is the imaginary part of x, m_R is the mean of x_R, m_I is the mean of x_I, σ_R^2 is the variance of x_R, σ_I^2 is the variance of x_I, and ρ is the correlation coefficient between x_R and x_I [42].

III. Non-coherent Detection

From (1), the conventional coherent detector can be derived as a minimum distance detector

$$\hat{x}_{\text{MD-C}} = \arg_x \min\{|y - hx|^2\}. \tag{11}$$

This detector assumes knowledge of the channel gain h. If this knowledge is not available or not used to save cost, the PDF of the received signal in (1) is $f(y) = \frac{1}{\pi(\sigma_n^2 + \sigma_h^2|x|^2)} e^{-\frac{|y|^2}{\sigma_n^2 + \sigma_h^2|x|^2}}$. Note that the PDF of y is conditioned on x but this conditioning is omitted for simplicity here and in the following. Thus, the conventional non-coherent ML detector can be derived as

$$\begin{aligned}\hat{x}_{\text{ML-C}} &= \arg_x \min\left\{\ln[\sigma_n^2 + \sigma_h^2|x|^2]\right. \\ &\quad \left. + \frac{|y|^2}{\sigma_n^2 + \sigma_h^2|x|^2}\right\}.\end{aligned} \tag{12}$$

For on-off keying (OOK), it can be shown that the detector in (12) is equivalent to the energy detector, which is widely used in low-cost applications [43], [44]. Next, we will derive the new detectors for hardware impaired signals.

A. AD Only

In this case, the received signal is given by (2). Using (2), the approximate ML non-coherent detector is obtained in the Appendix as

$$\begin{aligned}\hat{x}_{\text{AML-AD}} &= \arg_x \max\left\{\sum_{k=0}^{\infty} \frac{|y^* x|^{2k} (\sigma_h |y|)^{-k} e^{-\frac{|x|^2}{(\sigma_t^2 + \sigma_r^2)P}}}{(k!)^2 [(\sigma_t^2 + \sigma_r^2)P]^{3k/2}}\right. \\ &\quad \left. K_{-k}\left(\frac{2|y|}{\sqrt{\sigma_h^2(\sigma_t^2 + \sigma_r^2)P}}\right)\right\},\end{aligned} \tag{13}$$

where $K_a(x) = \frac{\pi}{2}\frac{I_{-a}(x) - I_a(x)}{\sin(a\pi)}$ is the a-th order modified Bessel function of the second type and $I_a(x) = \sum_{m=0}^{\infty} \frac{(x/2)^{2m+a}}{m!\Gamma(m+a+1)}$ is the a-th order modified Bessel function of the first type [45, eq. (8.406.1)].

To simplify the non-coherent detection, one can approximate y as a Gaussian random variable with mean zero and variance $\sigma_n^2+\sigma_h^2|x|^2+\sigma_h^2(\sigma_t^2+\sigma_r^2)P$. Thus,

$$f(y)\approx\frac{e^{-\frac{|y|^2}{\sigma_n^2+\sigma_h^2|x|^2+\sigma_h^2(\sigma_t^2+\sigma_r^2)P}}}{\pi[\sigma_n^2+\sigma_h^2|x|^2+\sigma_h^2(\sigma_t^2+\sigma_r^2)P]}, \tag{14}$$

and the Gaussian approximation (GA) non-coherent detector can be derived from (14) as

$$\begin{aligned}\hat{x}_{\text{GA-AD}} &= \arg_x\min\Big\{\ln[\sigma_n^2+\sigma_h^2|x|^2+\sigma_h^2(\sigma_t^2+\sigma_r^2)P]\\ &\quad+\frac{|y|^2}{\sigma_n^2+\sigma_h^2|x|^2+\sigma_h^2(\sigma_t^2+\sigma_r^2)P}\Big\}.\end{aligned} \tag{15}$$

It can be easily verified that for OOK, this detector becomes an energy detector. Also, the conventional non-coherent detector in (12) is a special case of (15) when there is no AD at either transmitter or receiver so that $\sigma_t^2=\sigma_r^2=0$.

For later comparison, the optimal coherent detector in the presence of AD is derived from (2) as

$$\hat{x}_{\text{OP-AD}}=\arg_x\min\{|y-hx|^2\}. \tag{16}$$

B. IQI Only

In this case, the received signal is given by (3). Denote $U=U_R+jU_I=hx_q+n=h(G_1x+G_2^*x^*)+n$. When h is unknown in the non-coherent detection, U is a complex Gaussian random variable with $U\sim\mathcal{CN}(0,\sigma_U^2)$ where $\sigma_U^2=\sigma_h^2|G_1x+G_2^*x^*|^2+\sigma_n^2$, as both h and n are Gaussian. One has from (3)

$$\begin{aligned}y &= y_R+jy_I=(K_1^RU_R-K_1^IU_I+K_2^RU_R+K_2^IU_I)\\ &\quad+j(K_1^RU_I+K_1^IU_R+K_2^IU_R-K_2^RU_I),\end{aligned} \tag{17}$$

where K_1^R, K_1^I, K_2^R, K_2^I are the real and imaginary parts of K_1 and K_2, respectively.

From (17), one has $E\{y_R\}=0$ and

$$\begin{aligned}\alpha_{yR}^2 &= E\{(K_1^RU_R-K_1^IU_I+K_2^RU_R+K_2^IU_I)^2\}\\ &= |K_1+K_2^*|^2\frac{\sigma_U^2}{2}=\frac{\sigma_U^2}{2}.\end{aligned} \tag{18}$$

Also, one has $E\{y_I\}=0$ and

$$\begin{aligned}\alpha_{yI}^2 &= E\{(K_1^RU_I+K_1^IU_R+K_2^IU_R-K_2^RU_I)^2\}\\ &= |K_1-K_2^*|^2\frac{\sigma_U^2}{2}=\zeta_R^2\frac{\sigma_U^2}{2}.\end{aligned} \tag{19}$$

Finally, the correlation coefficient between y_R and y_I is

$$\rho_y=\frac{E\{y_Ry_I\}}{\sigma_{yR}\sigma_{yI}}=\frac{2Im\{K_1K_2\}\sigma_U^2}{\zeta_R\sigma_U^2}=-\sin(\phi_R). \tag{20}$$

Thus, the received signal in (3) is an improper Gaussian random variable, as the correlation between its real and imaginary parts is not zero. Using (18) - (20) in (10) and after some manipulations, the non-coherent ML detector is derived as

$$\begin{aligned}\hat{x}_{\text{ML-IQI}} &= \arg_x\min\big\{\ln[\sigma_h^2|G_1x+G_2^*x^*|^2+\sigma_n^2]\\ &\quad+\frac{y_R^2+\frac{y_I^2}{\zeta_R^2}+\frac{2\sin(\phi_R)y_Ry_I}{\zeta_R}}{\cos^2(\phi_R)[\sigma_h^2|G_1x+G_2^*x^*|^2+\sigma_n^2]}\Big\}.\end{aligned} \tag{21}$$

Comparing (21) with (12), one sees that the conventional non-coherent detector is a special case of the new non-coherent detector when $\phi_T=\phi_R=0$ and $\zeta_T=\zeta_R=1$ so that there is no IQI at either the transmitter or the receiver.

For comparison, the optimal coherent detector is also given here. From (5), $z=z_R+jz_I$ is an improper Gaussian random variable with $E\{z\}=0$ and

$$\alpha_{zR}^2=E\{z_R^2\}=\frac{\sigma_n^2}{2}, \tag{22a}$$

$$\alpha_{zI}^2=E\{z_I^2\}=\zeta_R^2\frac{\sigma_n^2}{2}, \tag{22b}$$

$$\rho_z=-\sin(\phi_R), \tag{22c}$$

by using the same method as before. Denote $\Lambda_R=Re\{gx+fx^*\}$ and $\Lambda_I=Im\{gx+fx^*\}$, where $Re\{\cdot\}$ takes the real part of a complex number and $Im\{\cdot\}$ takes the imaginary part of a complex number. After some manipulations, the optimal coherent detector is

$$\begin{aligned}\hat{x}_{\text{OP-IQI}} &= \arg_x\min\Big\{(y_R-\Lambda_R)^2+\frac{(y_I-\Lambda_I)^2}{\zeta_R^2}\\ &\quad+\frac{2\sin(\phi_R)(y_R-\Lambda_R)(y_I-\Lambda_I)}{\zeta_R}\Big\}.\end{aligned} \tag{23}$$

This detector has also been derived in [28] and [32].

C. AD and IQI

This is the most complicated case. In this case, the received signal is given by (6) suffering from AD and IQI at both transmitter and receiver. So this is also the most general case. In this case, the approximate ML non-coherent detector is derived in the Appendix as

$$\begin{aligned}&\hat{x}_{\text{AML-ADIQI}}\\ &= \arg_x\max\Bigg\{\sum_{k=0}^{\infty}\frac{|G_1x+G_2^*x^*|^{2k}e^{-\frac{|G_1x+G_2^*x^*|^2}{(\sigma_t^2+\sigma_r^2)P'}}}{(k!)^2[(\sigma_t^2+\sigma_r^2)P']^{3k/2}}\\ &\quad\cdot\frac{(y_R^2+\frac{y_I^2}{\zeta_R^2}+\frac{2\sin(\phi_R)y_Ry_I}{\zeta_R})^{k/2}}{\cos^k(\phi_R)\sigma_h^k}\\ &\quad\cdot K_k\left(\frac{2\sqrt{(}y_R^2+\frac{y_I^2}{\zeta_R^2}+\frac{2\sin(\phi_R)y_Ry_I}{\zeta_R})}{\sqrt{\cos^2(\phi_R)\sigma_h^2(\sigma_t^2+\sigma_r^2)P'}}\right)\Bigg\}.\end{aligned} \tag{24}$$

To simplify the non-coherent detection, one can also approximate y_q as a Gaussian random variable with mean zero and variance $\sigma_n^2+\sigma_e^2\sigma_h^2+\sigma_h^2|G_1x+G_2^*x^*|^2$, where σ_e^2 is the variance of the AD e given by $\sigma_e^2=(\sigma_t^2+\sigma_r^2)P'$. Since $y=K_1y_q+K_2y_q^*$, y is an improper Gaussian random variable with $E\{y\}=0$ and

$$\alpha_{yR}^2=\frac{\sigma_n^2+|G_1x+G_2^*x^*|^2\sigma_h^2+\sigma_e^2\sigma_h^2}{2}, \tag{25a}$$

$$\alpha_{yI}^2=\zeta_R^2\frac{\sigma_n^2+|G_1x+G_2^*x^*|^2\sigma_h^2+\sigma_e^2\sigma_h^2}{2}, \tag{25b}$$

$$\rho_y=-\sin(\phi_R). \tag{25c}$$

Thus, the PDF of y can be derived as

$$f(y) \approx \frac{e^{-\frac{y_R^2+\frac{y_I^2}{\zeta_R^2}+\frac{2\sin(\phi_R)}{\zeta_R}y_Ry_I}{\cos^2(\phi_R)\alpha_{yR}^2}}}{2\pi\zeta_R\cos(\phi_R)\alpha_{yR}^2}. \quad (26)$$

Finally, the GA non-coherent detector is derived from (26) as

$$\begin{aligned}&\hat{x}_{\text{GA-ADIQI}}\\ &= \arg_x \min\Big\{\ln[\sigma_n^2+\sigma_h^2|G_1x+G_2^*x^*|^2+\sigma_h^2\sigma_e^2]\\ &+\frac{y_R^2+\frac{y_I^2}{\zeta_R^2}+\frac{2\sin(\phi_R)}{\zeta_R}y_Ry_I}{\cos^2(\phi_R)[\sigma_n^2+\sigma_h^2|G_1x+G_2^*x^*|^2+\sigma_h^2\sigma_e^2]}\Big\}. \quad (27)\end{aligned}$$

This non-coherent detector is much simpler than the approximate ML detector in (24).

For later comparison, the optimal coherent detector with known channel gain is also given here. From (9), when h is known, one has $eh+n$ following $\mathcal{CN}(0,\sigma_n^2+(\sigma_t^2+\sigma_r^2)P'|h|^2)$. Thus, $w=K_1(eh+n)+K_2(eh+n)^*$ is an improper Gaussian random variable with $E\{w\}=0$ and

$$\alpha_{wR}^2=\frac{\sigma_n^2+(\sigma_t^2+\sigma_r^2)P'|h|^2}{2}, \quad (28a)$$

$$\alpha_{wI}^2=\zeta_R^2\frac{\sigma_n^2+(\sigma_t^2+\sigma_r^2)P'|h|^2}{2}, \quad (28b)$$

$$\rho_w=-\sin(\phi_R). \quad (28c)$$

The derivation is similar to before. This gives the optimal coherent detector as

$$\begin{aligned}\hat{x}_{\text{OP-ADIQI}} &= \arg_x\min\Big\{(y_R-\Lambda_R)^2+\frac{(y_I-\Lambda_I)^2}{\zeta_R^2}\\ &+\frac{2\sin(\phi_R)(y_R-\Lambda_R)(y_I-\Lambda_I)}{\zeta_R}\Big\}. \quad (29)\end{aligned}$$

This detector has also been derived in [28] before. It has the same form as the detector in (23), except that the received signal y_R and y_I in (29) are determined by (6), while those in (23) are determined by (4). The performances of these detectors will be examined and compared later.

Remark. *Similar to the conventional non-coherent detector in (12), the proposed approximate ML and GA non-coherent detectors in (13), (15), (21), (24) and (27) remove the phase information of the transmitted signal x by squaring it. Thus, these detectors are only applicable to amplitude modulation, frequency modulation and position modulation [46], [47]. For phase modulation, it is well-known that its non-coherent detection requires differential encoding at the transmitter, which is not discussed here [46]. Nevertheless, amplitude modulation, frequency modulation and position modulation are widely used in low-cost low-power applications. For example, energy detection is a type of OOK that is very important for spectrum sensing in cognitive radios [49]. It is also widely used in ambient backscatter communications [50]. For ultra-wide bandwidth systems, pulse position modulation is one of the two main modulation schemes studied [48]. Our proposed non-coherent detectors can be used in these applications.*

Remark. *For low-cost low-power applications, performance is often less important than cost. Hence, single-antenna and single-carrier implementation is more likely to be used than multi-antenna and multi-carrier implementation to save spectral and energy costs. For example, in LoRa for Internet-of-Things, single antenna and single carrier are used by remote devices [51]. In surveillance, passive radar can also use single-antenna and single-carrier GSM signals for target detection [52], [53]. Thus, this work assumes single-antenna and single-carrier in the derivation.*

IV. Channel Estimation

Since the coherent detectors require channel knowledge, in this section, channel estimation of hardware impaired signals will be studied. Assume that L known pilot symbols are used to estimate the channel gain h. When there is no HWI, the l-th received signal is given by

$$y_l=hx_l+n_l, \quad (30)$$

where $l=1,2,\cdots,L$, x_l is the l-th pilot and its value is known, n_l is the noise in the l-th sample following the same distribution as n in (1), and h is the channel gain to be estimated. The conventional ML estimator for h ignoring HWI is given in [54] as

$$\hat{h}=\frac{\sum_{l=1}^L y_lx_l^*}{\sum_{l=1}^L|x_l|^2}. \quad (31)$$

When there is only AD, the l-th received signal is given by

$$y_l=h(x_l+d_l)+n_l, \quad (32)$$

where d_l and n_l are the AD and noise in the l-th sample following the same distributions as d and l in (2), respectively, and other symbols are defined as before. Similarly, when there is only IQI, the l-th received signal is given by

$$y_l=K_1(hx_{ql}+n_l)+K_2(hx_{ql}+n_l)^*, \quad (33)$$

where $x_{ql}=G_1x_l+G_2^*x_l^*$ and n_l has the same distribution as n in (3), and when there are both AD and IQI, the l-th received signal is given by

$$y_l=K_1y_{ql}+K_2y_{ql}^*, \quad (34)$$

where $y_{ql}=h(x_{ql}+e_l)+n_l$ and e_l, n_l have the same distributions as e and n in (7), respectively.

A. AD Only

We study the ML estimation first. In this case, the joint PDF of the L received samples is derived from (32) as

$$f(\mathbf{y}|h)=\frac{e^{-\frac{1}{\sigma_n^2+(\sigma_t^2+\sigma_r^2)P|h|^2}\sum_{l=1}^L|y_l-hx_l|^2}}{\pi^L[\sigma_n^2+(\sigma_t^2+\sigma_r^2)P|h|^2]^L}. \quad (35)$$

Since $h=re^{\theta}$, one has the log-likelihood function as

$$\begin{aligned}\ln f(\mathbf{y}|r,\theta) &= -L\ln\{\pi[\sigma_n^2+(\sigma_t^2+\sigma_r^2)Pr^2]\}\\ &-\frac{\sum_{l=1}^L|y_l|^2}{\sigma_n^2+(\sigma_t^2+\sigma_r^2)Pr^2}-\frac{r^2\sum_{l=1}^L|x_l|^2}{\sigma_n^2+(\sigma_t^2+\sigma_r^2)Pr^2}\\ &+\frac{2r\sum_{l=1}^L|y_lx_l^*|\cos(\theta_l-\theta)}{\sigma_n^2+(\sigma_t^2+\sigma_r^2)Pr^2}, \quad (36)\end{aligned}$$

where $\theta_l = \tan^{-1}\frac{Re\{y_l x_l^*\}}{Im\{y_l x_l^*\}}$ is the phase angle of $y_l x_l^*$ and $\tan^{-1}(\cdot)$ is the inverse tangent function. Taking the first-order derivative of the log-likelihood function with respect to θ, one has

$$\frac{\partial \ln f(\mathbf{y}|r,\theta)}{\partial\theta} = \frac{2r\sum_{l=1}^{L}|y_l x_l^*|\sin(\theta_l-\theta)}{\sigma_n^2+(\sigma_t^2+\sigma_r^2)Pr^2} = 0, \quad (37)$$

which can be solved to give the ML estimator for θ as

$$\hat{\theta}_{\text{ML}} = \tan^{-1}\frac{\sum_{l=1}^{L}|y_l x_l^*|\sin(\theta_l)}{\sum_{l=1}^{L}|y_l x_l^*|\cos(\theta_l)}. \quad (38)$$

Similarly, the ML estimator for r can be obtained by taking the first-order derivative of the log-likelihood function with respect to r and setting the derivative to zero, which gives

$$\begin{aligned}&(\sigma_t^2+\sigma_r^2)Pr^3 + \frac{1}{L}\sum_{l=1}^{L}|y_l x_l^*|\cos(\theta_l-\hat{\theta}_{ML})r^2\\ &-(\frac{1}{L}\sum_{l=1}^{L}|y_l|^2-\sigma_n^2-\frac{\sigma_n^2\sum_{l=1}^{L}|x_l|^2}{L(\sigma_t^2+\sigma_r^2)P})r\\ &-\frac{\sigma_n^2}{L(\sigma_t^2+\sigma_r^2)P}\sum_{l=1}^{L}|y_l x_l^*|\cos(\theta_l-\hat{\theta}_{ML}) = 0. \quad (39)\end{aligned}$$

This is a third-order polynomial whose solutions are quite complicated. To simplify the estimation, assuming that $\sigma_n^2 << (\sigma_t^2+\sigma_r^2)P$, one has

$$r^2 + \frac{\sum_{l=1}^{L}|y_l x_l^*|\cos(\theta_l-\hat{\theta}_{\text{ML}})}{L(\sigma_t^2+\sigma_r^2)P}r - \frac{\sum_{l=1}^{L}|y_l|^2}{L(\sigma_t^2+\sigma_r^2)P} = 0,$$

which is solved to give the approximate ML estimator for r as

$$\begin{aligned}\hat{r}_{\text{ML}} &= -\frac{\sum_{l=1}^{L}|y_l x_l^*|\cos(\theta_l-\hat{\theta}_{\text{ML}})}{2L(\sigma_t^2+\sigma_r^2)P} \quad (40)\\ &+ \sqrt{(\frac{\sum_{l=1}^{L}|y_l x_l^*|\cos(\theta_l-\hat{\theta}_{\text{ML}})}{2L(\sigma_t^2+\sigma_r^2)P})^2+\frac{\sum_{l=1}^{L}|y_l|^2}{L(\sigma_t^2+\sigma_r^2)P}}.\end{aligned}$$

Finally, the ML estimator for h is

$$\hat{h}_{\text{ML}} = \hat{r}_{\text{ML}}e^{j\hat{\theta}_{\text{ML}}}, \quad (41)$$

where $\hat{r}_{\text{ML}}$ is given by (40) and θ_{ML} is given by (38).

The ML estimator for r in (40) is complicated. A simpler estimator can be obtained by using the moment-based (MB) method. In this case, from (2), one has the second-order moment of y as

$$E\{|y|^2\} = |h|^2E\{|x|^2\} + |h|^2E\{|d|^2\} + E\{|n|^2\}, \quad (42)$$

where $E\{|d|^2\} = (\sigma_t^2+\sigma_r^2)P$, $E\{|n|^2\} = \sigma_n^2$, $E\{|y|^2\} \approx \frac{1}{L}\sum_{l=1}^{L}|y_l|^2$ and $E\{|x|^2\} \approx \frac{1}{L}\sum_{l=1}^{L}|x_l|^2$. Thus, the MB estimator for r is

$$\hat{r}_{\text{MB}} = \sqrt{\frac{\frac{1}{L}\sum_{l=1}^{L}|y_l|^2-\sigma_n^2}{\frac{1}{L}\sum_{l=1}^{L}|x_l|^2+(\sigma_t^2+\sigma_r^2)P}}. \quad (43)$$

Also, a mixed ML-MB estimator for h is

$$\hat{h}_{\text{ML-MB}} = \hat{r}_{\text{MB}}e^{j\theta_{\text{ML}}}, \quad (44)$$

where $\hat{r}_{\text{MB}}$ is given by (43) and θ_{ML} is given by (38).

A pure MB estimator for h can also be derived by using the first-order moment of y as

$$E\{yx^*\} = hE\{|x|^2\} + hE\{dx^*\} + E\{nx^*\} = hE\{|x|^2\}, \quad (45)$$

as d and n have zero mean. Thus,

$$\hat{h}_{\text{MB}} = \frac{\sum_{l=1}^{L}y_l x_l^*}{\sum_{l=1}^{L}|x_l|^2}. \quad (46)$$

One sees that, in this specific case, $\hat{h}_{\text{MB}}$ in (46) happens to be the same as the conventional ML estimator in (31). In the general case, they are different, and it can be proved that the ML estimator is asymptotically efficient while the MB estimator is not [55]. However, in this specific case, the MB estimator is also asymptotically efficient.

B. IQI Only

From (33) and (4), y_l can be rewritten as $y_l = y_{Rl}+jy_{Il} = gx_l + fx_l^* + z_l$, where $z_l = K_1n_l + K_2n_l^*$ is an improper Gaussian random variable whose statistics are given by (22). Thus, y_l also follows an improper Gaussian distribution only with non-zero mean $gx_l + fx_l^*$. Specifically, denoting $h = h_R + jh_I$ and $\Lambda_l = \Lambda_{Rl} + j\Lambda_{Il} = gx_l + fx_l^*$, one has

$$\Lambda_{Rl} = B_{l1}h_R + B_{l2}h_I, \quad (47a)$$

$$\Lambda_{Il} = B_{l3}h_R + B_{l4}h_I, \quad (47b)$$

with

$$B_{l1} = Re\{K_1G_1x_l + K_1G_2^*x_l^* + K_2G_2x_l + K_2G_1^*x_l^*\}, \quad (48a)$$

$$B_{l2} = Im\{-K_1G_1x_l - K_1G_2^*x_l^* + K_2G_2x_l + K_2G_1^*x_l^*\}, \quad (48b)$$

$$B_{l3} = Im\{K_1G_1x_l + K_1G_2^*x_l^* + K_2G_2x_l + K_2G_1^*x_l^*\}, \quad (48c)$$

$$B_{l4} = Re\{K_1G_1x_l + K_1G_2^*x_l^* - K_2G_2x_l - K_2G_1^*x_l^*\}. \quad (48d)$$

The joint PDF of all L samples can be derived as

$$\begin{aligned}f(\mathbf{y}|h_R,h_I) &= \frac{e^{-\frac{1}{2(1-\rho_z^2)}\sum_{l=1}^{L}[\frac{(y_{Rl}-\Lambda_{Rl})^2}{\alpha_{zR}^2}+\frac{(y_{Il}-\Lambda_{Il})^2}{\alpha_{zI}^2}]}}{[2\pi\alpha_{zR}\alpha_{zI}\sqrt{1-\rho_z^2}]^L}\\ &\cdot e^{\frac{1}{2(1-\rho_z^2)}\sum_{l=1}^{L}\frac{2\rho_z(y_{Rl}-\Lambda_{Rl})(y_{Il}-\Lambda_{Il})}{\alpha_{Rl}\alpha_{Il}}}, \quad (49)\end{aligned}$$

where Λ_{Rl} and Λ_{Il} are given by (47), α_{zR}, α_{zI} and ρ_z are given by (22). By taking the first-order derivatives of $f(\mathbf{y}|h_R,h_I)$ with respect to h_R and h_I and setting the derivatives to zero, two equations can be obtained as

$$\begin{aligned}&\sum_{l=1}^{L}(\frac{2B_{l1}^2}{\alpha_{zR}^2}+\frac{2B_{l3}^2}{\alpha_{zI}^2}-\frac{4\rho_z B_{l1}B_{l3}}{\alpha_{zR}\alpha_{zI}})h_R \quad (50a)\\ &+\sum_{l=1}^{L}(\frac{2B_{l1}B_{l2}}{\alpha_{zR}^2}+\frac{2B_{l3}B_{l4}}{\alpha_{zI}^2}-\frac{2\rho_z(B_{l2}B_{l3}+B_{l1}B_{l4})}{\alpha_{zR}\alpha_{zI}})h_I\\ &=\sum_{l=1}^{L}(\frac{2B_{l1}}{\alpha_{zR}^2}-\frac{2\rho_z B_{l3}}{\alpha_{zR}\alpha_{zI}})y_{Rl}+\sum_{l=1}^{L}(\frac{2B_{l3}}{\alpha_{zI}^2}-\frac{2\rho_z B_{l1}}{\alpha_{zR}\alpha_{zI}})y_{Il},\end{aligned}$$

$$\sum_{l=1}^{L}\left(\frac{2B_{l1}B_{l2}}{\alpha_{zR}^2}+\frac{2B_{l3}B_{l4}}{\alpha_{zI}^2}-\frac{2\rho_z(B_{l2}B_{l3}+B_{l1}B_{l4})}{\alpha_{zR}\alpha_{zI}}\right)h_R$$
$$+\sum_{l=1}^{L}\left(\frac{2B_{l2}^2}{\alpha_{zR}^2}+\frac{2B_{l4}^2}{\alpha_{zI}^2}-\frac{4\rho_z B_{l2}B_{l4}}{\alpha_{zR}\alpha_{zI}}\right)h_I \quad (50b)$$
$$=\sum_{l=1}\left(\frac{2B_{l2}}{\alpha_{zR}^2}-\frac{2\rho_z B_{l4}}{\alpha_{zR}\alpha_{zI}}\right)y_{Rl}+\sum_{l=1}\left(\frac{2B_{l4}}{\alpha_{zI}^2}-\frac{2\rho_z B_{l2}}{\alpha_{zR}\alpha_{zI}}\right)y_{Il}.$$

Solving these two linear equations for h_R and h_I, the ML estimators can be derived as $\hat{h_R}$ and $\hat{h_I}$, respectively. Thus, the ML estimator for h in the case when there is only IQI is

$$\hat{h}_{\text{ML}}=\hat{h_R}+j\hat{h_I}, \quad (51)$$

where $\hat{h_R}$ and $\hat{h_I}$ are solutions to (50).

Next, we will derive the MB estimator for h. From (4), one has

$$E\{yx^*\}=\Lambda x^*, \quad (52)$$

which gives two linear equations for the real and imaginary parts as

$$Re\{\frac{1}{L}\sum_{l=1}^{L}y_l x_l^*\}=\frac{1}{L}\sum_{l=1}^{L}B_{l1}x_l^*h_R+\frac{1}{L}\sum_{l=1}^{L}B_{l2}x_l^*h_I, \quad (53a)$$

$$Im\{\frac{1}{L}\sum_{l=1}^{L}y_l x_l^*\}=\frac{1}{L}\sum_{l=1}^{L}B_{l3}x_l^*h_R+\frac{1}{L}\sum_{l=1}^{L}B_{l4}x_l^*h_I. \quad (53b)$$

These two equations can be solved to give the MB estimator for h as

$$\hat{h}_{\text{MB}}=\hat{h_R}+j\hat{h_I}, \quad (54)$$

where $\hat{h_R}$ and $\hat{h_I}$ are solutions to (53).

C. AD and IQI

When both AD and IQI exist, the received sample is given by (34). It can be shown that the ML estimator for h is very difficult to obtain, as one has to solve two nonlinear equations for h_R and h_I. Thus, we only derive the MB estimator in this case. From (8), one has

$$E\{yx^*\}=\Lambda x^*, \quad (55)$$

as the mean of wx^* is also zero. One sees that (55) has the same form as (52), except that the sample has both AD and IQI now. Thus, the MB estimator for h in the presence of both IQI and AD has the same form as (54), except that y_l is determined by (34).

V. Numerical Results and Discussion

In this section, numerical examples are presented by computer simulation. In the examination, we set $P=1$, $\sigma_h^2=1$, $\phi_T=\phi_R=5°$, $\zeta_T=\zeta_R=\zeta=0.835$ or 1.670, and run 10^6 trials. The values of $\zeta=0.835$ and $\phi_T=\phi_R=5°$ were chosen according to [28] to give a typical image rejection ratio of 20 dB [2]. The value of $\zeta=1.67$ was chosen to examine the effect of ζ by doubling 0.835. Other values are also possible. For the approximate ML non-coherent detectors, the infinite series is truncated to the first 50 terms. We consider OOK.

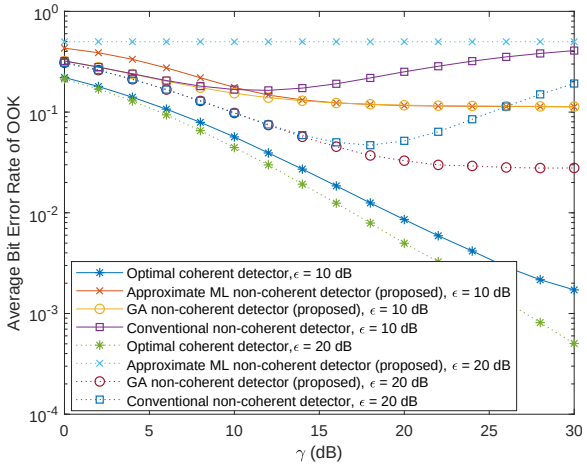

Fig. 1. Bit error rate of OOK with AD only.

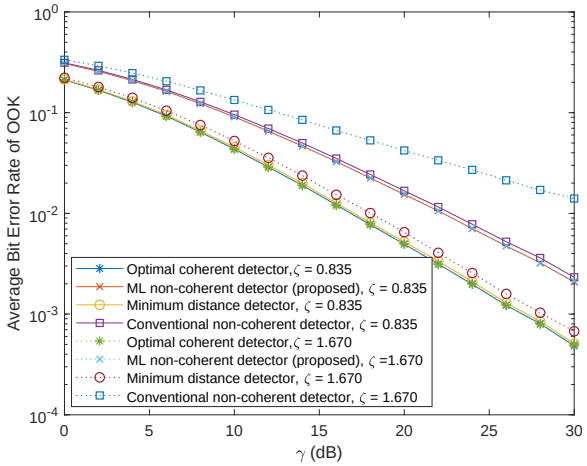

Fig. 2. Bit error rate of OOK with IQI only.

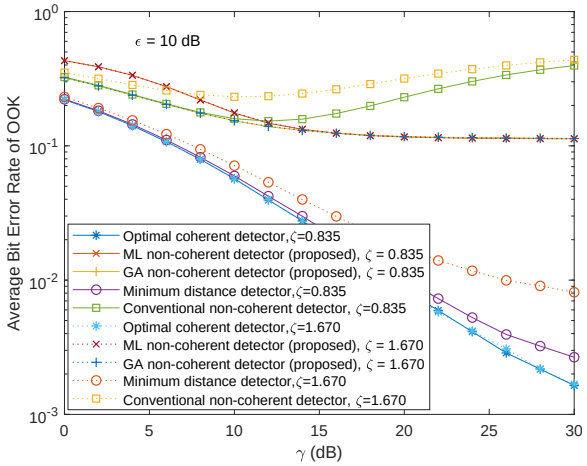

Fig. 3. Bit error rate of OOK with both AD and IQI.

Define $\gamma = \frac{\sigma_h^2}{\sigma_n^2}$ as the SNR. For the detectors, the error rate is studied. For channel estimators, the MSE is studied.

Figs. 1 - 3 show the performances of the non-coherent detectors using OOK with AD only, with IQI only, or with both AD and IQI, respectively. The optimal coherent detector is also given as a benchmark. From Fig. 1, one sees that the optimal coherent detector performs the best, as expected. Among the non-coherent detectors, the GA non-coherent detector is the best. It approaches a lower limit as γ increases. This is caused by the AD, as can be seen from (2), where the AD increases with h. For the conventional non-coherent detector, its error rate first decreases then increases with γ. The conventional non-coherent detector is derived by assuming that the received signal is Gaussian. At small γ, the Gaussian noise is strong and therefore, the Gaussianity of the received signal in (2) is high. Consequently, the error rate decreases with γ. As γ keeps increasing, the noise becomes weak so that the AD starts to dominate. However, when the AD dominates, the received signal is not Gaussian any more, as $d * h$ is not Gaussian. Hence, the conventional non-coherent detector based on the Gaussian assumption starts to deteriorate when γ keeps increasing. For the approximate ML non-coherent detector, when $\epsilon = 10dB$, its performance is identical with the GA non-coherent detector when γ is larger than 15 dB. Its performance when $\epsilon = 20dB$ is worse than that when $\epsilon = 10dB$, because its derivation is based on the approximation of $\sigma_n^2 << (\sigma_t^2 + \sigma_r^2)P$ from (58) but when the SDR $\epsilon = \frac{\sigma_h^2}{(\sigma_t^2+\sigma_r^2)P}$ is large, $(\sigma_t^2+\sigma_r^2)P$ is small for fixed σ_h^2 so that the approximation is no longer valid. This leads to large approximation errors in the approximate detector and thus poor performance when $\epsilon = 20dB$.

Also, from Fig. 2, the new ML non-coherent detector is slightly better than the conventional non-coherent detector when $\zeta = 0.835$. When ζ increases to 1.670, the performance of the new ML non-coherent detector almost does not change, while the conventional non-coherent detector degrades a lot so that at an error rate of 10^{-2}, the new non-coherent detector is almost 8 dB better than the conventional one. Similar observations can be made from Fig. 3, where the SDR is fixed at 10 dB, while ζ changes from 0.835 to 1.670. One sees that the new ML and GA non-coherent detectors are not sensitive to the change of the IQI ζ at all, so is the optimal coherent detector. On the other hand, both the conventional non-coherent detector and the minimum distance detector degrade considerably when ζ increases. Moreover, the error rate of the conventional non-coherent first decreases then increases, similar to Fig. 1.

Figs. 4 - 6 show the MSEs of the derived channel estimators. One sees that all the MSEs decrease when the sample size L increases, or when the SNR γ increases. When there is AD only, from Fig. 4, all MSEs approach lower limits with increasing γ, caused by the AD as can be seen from (32). Among the new estimators, the MB estimator has the same performance as the conventional ML estimator, as expected, as (46) is the same as (31). Both the ML estimator in (41) and ML-MB estimator in (44) are worse than the conventional ML estimator when γ is small and better than it when γ is large. When γ is small, the Gaussian noise dominates so that the Gaussian assumption based on which the conventional

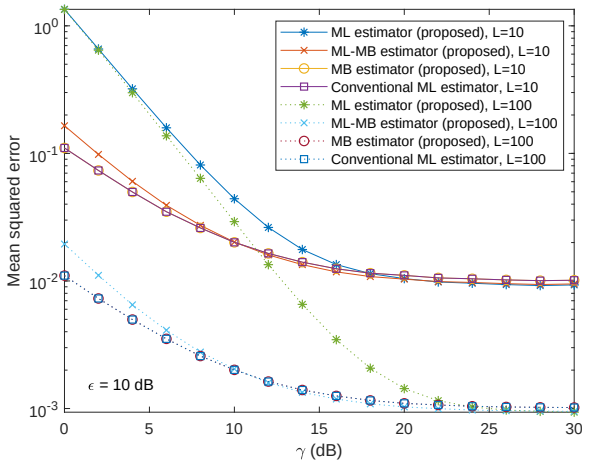

Fig. 4. Mean squared error for estimators with AD only.

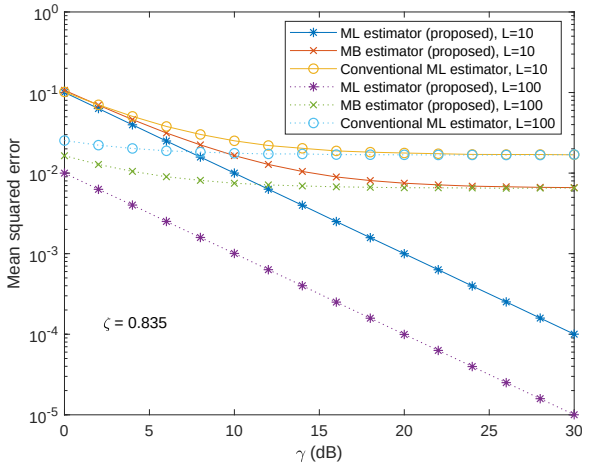

Fig. 5. Mean squared error for estimators with IQI only.

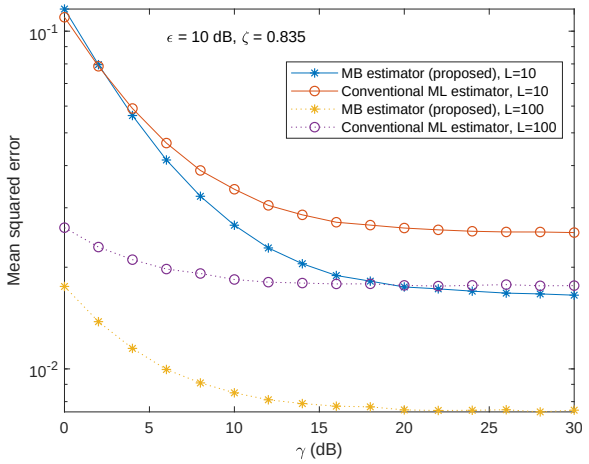

Fig. 6. Mean squared error for estimators with both AD and IQI.

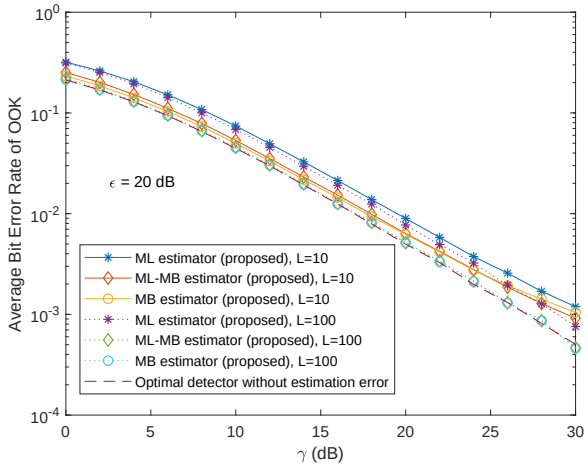

Fig. 7. Bit error rate of OOK with channel estimation error in AD.

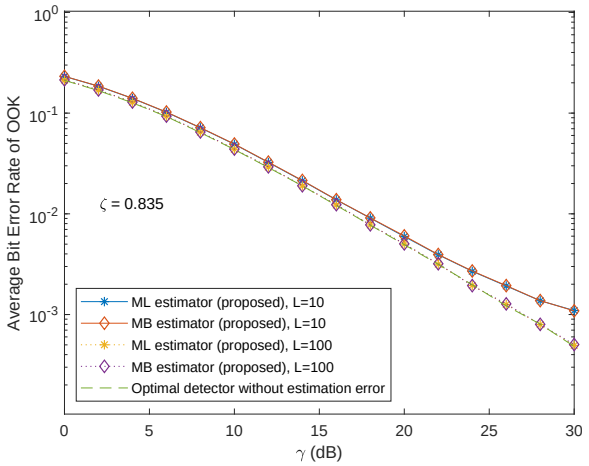

Fig. 8. Bit error rate of OOK with channel estimation error in IQI.

estimator is derived will be valid. Under the same conditions, since the ML-MB estimator in (44) uses the second-order moment and the ML estimator in (41) ignores the noise, they under-perform the conventional estimator using the first-order moment. When γ increases, the AD dominates so that the Gaussian assumption based on which the conventional estimator is derived will no longer be valid. Hence, the ML-MB estimator and the ML estimator start to outperform it. Also, the ML-MB estimator outperforms the ML estimator, as the ML estimator ignores the noise and hence incurs large approximation errors when γ is small and the noise is strong.

Also, when there is IQI only, from Fig. 4, the new ML estimator in (51) is always the best. In some reasonable conditions, such as when $\gamma = 16\ dB$ and $L = 100$, the new ML estimator is about 100 times better than the conventional ML estimator. The new MB estimator in (54) is also better than the conventional ML estimator. Moreover, the MB estimator and the conventional ML estimator have an error floor, while the new ML estimator does not. When there are both AD and IQI, from Fig. 6, the new MB estimator always outperforms the conventional ML estimator. Both have error floors but the new estimator has a lower floor with less errors. In fact, the MSE of the new estimator when $L = 10$ is even lower than that of the conventional ML estimator when $L = 100$, for $\gamma > 20\ dB$.

Figs. 7 - 9 show the bit error rates of OOK using different channel estimators proposed for the optimal coherent detector in (16), (23) and (29), respectively. One sees from Fig. 7 that the ML-MB estimator in (44) and the MB estimator in (46) give almost identical performance to the detector with perfect channel knowledge, when $L = 100$. When $L = 10$, there is a gap between them and the perfect detector, and the gap increases with γ. For the ML estimator in (41), there is a considerable performance gap. Also, from Fig. 8, the ML estimator in (51) and the MB estimator in (54) have identical performance to the detector without estimation error when $L = 100$. The performance gap between $L = 10$ and $L = 100$ is also small, especially when γ is small. Finally, from Fig. 9, similar observations can be made, where $L = 100$

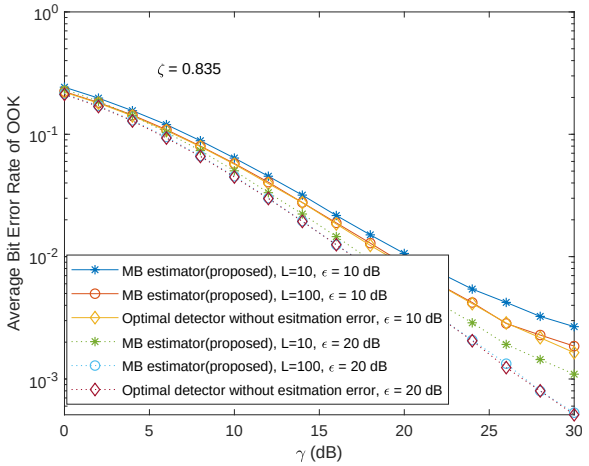

Fig. 9. Bit error rate of OOK with channel estimation error in both AD and IQI.

gives almost identical performance with perfect estimation. The performance difference is more sensitive to the sample size L than to the SDR ϵ.

Fig. 10 compares the coherent detector in (29) using channel estimates from (54) with the GA non-coherent detector in (27), when both AD and IQI occur. The coherent detector takes the energy penalty of pilots into account. If L pilots are used, the effective SNR of the coherent detector becomes $\frac{\gamma}{L+1}$. One sees that the GA non-coherent detector outperforms the coherent detector with estimated channel, when γ is small. As γ increases, the coherent detector with estimated channel becomes better than the GA non-coherent detector, as the GA detector suffers from an error floor. Also, for the coherent detector, $L = 10$ has a better performance than $L = 100$. This is because the energy penalty for $L = 100$ is larger than the accuracy improvement. Finally, the detection performance improves when ϵ increases, as expected. Fig. 11 compares the proposed detectors for OOK and 4-ary amplitude modulation (4-AM). As expected, 4-AM has poorer performance. In most low-power low-cost applications, reliability is more important than rate. Hence, binary modulation is preferable. Table I

TABLE I

COMPLEXITY COMPARISON

Detector/Estimator	Complexity
Conventional detector in (11)	one logarithm
Approximate ML in (12)	one Bessel, one infinite series, four powering, one exponential
GA in (14)	one logarithm
ML in (21)	one logarithm, conversion of complex signals to real and imaginary parts
Approximate ML in (24)	one Bessel, one infinite series, six powering, one exponential, conversion of complex signals to real and imaginary parts
GA in (27)	one logarithm, conversion of complex signals to real and imaginary parts
Conventional estimators	iterative, matrix operations
New estimators	one-shot, simple multiplications and additions

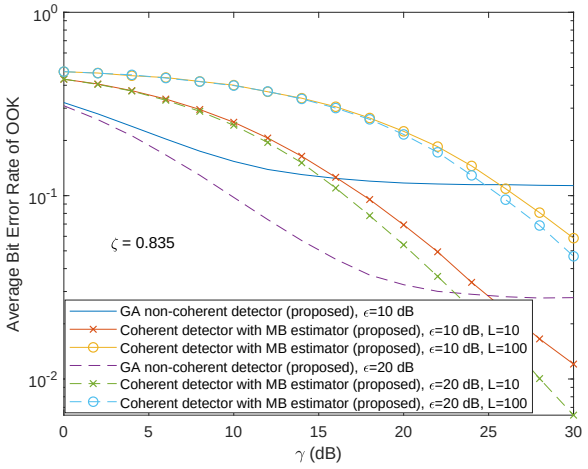

Fig. 10. Comparison of the coherent detector in (29) using the proposed MB estimator in (54) and the GA non-coherent detector in (27) with both AD and IQI.

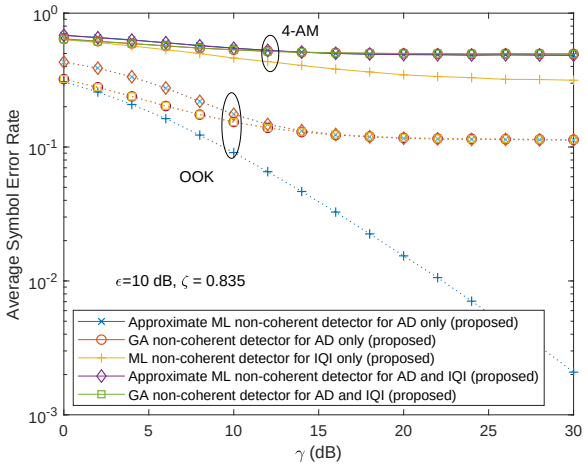

Fig. 11. Comparison of the proposed detectors for OOK and 4-AM.

compares the complexity of different detectors and estimators.

VI. CONCLUSION

We have proposed several new non-coherent detectors and channel estimators for hardware impaired signals suffering from either AD, or IQI or both. Numerical results have shown that the newly proposed non-coherent detectors outperform the conventional non-coherent detectors. These detectors are very useful for applications where low cost is preferred, as they do not require channel knowledge. Numerical results have also shown that the new channel estimators perform much better than the conventional ML estimators ignoring HWI. When multiple antennas are used, similar methods to [29] can be used. In this case, (8) will become [9, eq. (10)], where x, y and w become vectors with elements from different antennas, and g and f will become matrices that incorporate the channel and HWI matrix. The approximate ML non-coherent detector can be obtained by averaging the conditional joint PDF of the received signals, conditioned on the channel, over the channel matrix whose elements are independent to give the joint PDF as multi-variate Gaussian. The GA non-coherent detector can be directly derived by deriving the mean and variance of the received signal vector. The new ML estimators can also be obtained from the approximate joint likelihood function, while the MB estimator can be obtained from its first- and second-order moments. Due to the space limitation, they are not presented here.

APPENDIX DERIVATION OF (13) AND (24)

Using the ML method, the likelihood function conditioned on h can be derived from (2) as

$$f(y|h) = \frac{1}{\pi[\sigma_n^2 + (\sigma_t^2+\sigma_r^2)P|h|^2]} e^{-\frac{|y-hx|^2}{\sigma_n^2+(\sigma_t^2+\sigma_r^2)P|h|^2}}, \quad (56)$$

since y is a complex Gaussian random variable with mean hx and variance $\sigma_n^2 + (\sigma_t^2+\sigma_r^2)P|h|^2$. Denote $h = re^{j\theta}$. Since Rayleigh fading is assumed, one has the joint PDF of r and θ as $f(r,\theta) = \frac{r}{\pi\sigma_h^2} e^{-\frac{r^2}{\sigma_h^2}}$. Thus, the unconditional likelihood function is

$$\begin{aligned} f(y) &= \int_0^\infty \int_0^{2\pi} f(y|re^{j\theta}) f(r,\theta) d\theta dr \quad (57)\\ &= \int_0^\infty \int_0^{2\pi} \frac{re^{-\frac{r^2}{\sigma_h^2}}}{\pi^2\sigma_h^2[\sigma_n^2 + (\sigma_t^2+\sigma_r^2)Pr^2]} \\ &\quad \cdot e^{-\frac{|y|^2+r^2|x|^2-2r|y^*x|\cos(\Psi-\theta)}{\sigma_n^2+(\sigma_t^2+\sigma_r^2)Pr^2}} d\theta dr \\ &= \int_0^\infty \frac{2re^{-\frac{r^2}{\sigma_h^2}-\frac{|y|^2+r^2|x|^2}{\sigma_n^2+(\sigma_t^2+\sigma_r^2)Pr^2}}}{\pi\sigma_h^2[\sigma_n^2 + (\sigma_t^2+\sigma_r^2)Pr^2]} \\ &\quad \cdot I_0\left(\frac{2r|y^*x|}{\sigma_n^2 + (\sigma_t^2+\sigma_r^2)Pr^2}\right) dr, \end{aligned}$$

where Ψ is the phase angle of y^*x, $I_0(\cdot)$ is the zero-th order modified Bessel function of the first type [45, eq. (8.406.1)], and the last equation is obtained by integrating over θ using

[45, eq. (3.339)]. This integral cannot be solved. However, when $\sigma_n^2 << (\sigma_t^2+\sigma_r^2)P$, one has

$$\begin{aligned} f(y) &\approx \int_0^\infty \frac{2e^{-\frac{|x|^2}{(\sigma_t^2+\sigma_r^2)P}-\frac{|y|^2}{(\sigma_t^2+\sigma_r^2)Pr^2}-\frac{r^2}{\sigma_h^2}}}{\sigma_h^2\pi(\sigma_t^2+\sigma_r^2)Pr} \\ &\quad \cdot I_0\left(\frac{2|y^*x|}{(\sigma_t^2+\sigma_r^2)Pr}\right)dr \\ &= \frac{2e^{-\frac{|x|^2}{(\sigma_t^2+\sigma_r^2)P}}}{\sigma_h^2\pi(\sigma_t^2+\sigma_r^2)P}\sum_{k=0}^{\infty}\frac{|y^*x|^{2k}}{(k!)^2[(\sigma_t^2+\sigma_r^2)P]^{2k}} \\ &\quad \cdot \int_0^\infty \frac{e^{-\frac{|y|^2}{(\sigma_t^2+\sigma_r^2)Pr^2}-\frac{r^2}{\sigma_h^2}}}{r^{2k+1}}dr \\ &= \frac{2e^{-\frac{|x|^2}{(\sigma_t^2+\sigma_r^2)P}}}{\sigma_h^2\pi(\sigma_t^2+\sigma_r^2)P}\sum_{k=0}^{\infty}\frac{|y^*x|^{2k}(\sigma_h|y|)^{-k}}{(k!)^2[(\sigma_t^2+\sigma_r^2)P]^{3k/2}} \\ &\quad \cdot K_{-k}\left(\frac{2|y|}{\sqrt{\sigma_h^2(\sigma_t^2+\sigma_r^2)P}}\right), \end{aligned} \tag{58}$$

where the first equation is obtained by using the series expansion of the Bessel function [45, eq. (8.447.1)], and the second equation is obtained by using [45, eq. (3.478.4)]. In practice, this assumption holds when HWI dominates the channel distortion. This happens when the nonlinearity of the RF components are particularly high or when the receiver noise is very low. From (58), one has (13).

Similarly, from (7), y_q is a complex Gaussian random variable with $y_q \sim \mathcal{CN}(0, |G_1x+G_2^*x^*+e|^2\sigma_h^2+\sigma_n^2)$, conditioned on the AD e. Also, from (6), $y = y_R+jy_I = K_1y_q+K_2y_q^*$ and using the same method as before by expanding y to its real and imaginary parts, it can be shown that $E\{y_R\} = E\{y_I\} = 0$ and

$$\alpha_{yR}^2 = E\{y_R^2\} = \frac{\sigma_n^2+|G_1x+G_2^*x^*+e|^2\sigma_h^2}{2}, \tag{59a}$$

$$\alpha_{yI}^2 = E\{y_I^2\} = \zeta_R^2\frac{\sigma_n^2+|G_1x+G_2^*x^*+e|^2\sigma_h^2}{2}, \tag{59b}$$

$$\rho_y = -\sin(\phi_R). \tag{59c}$$

Thus, y is an improper Gaussian random variable, and the PDF of y, conditioned on e, can be derived using (59) as

$$f(y|e) = \frac{e^{-\frac{y_R^2+\frac{y_I^2}{\zeta_R^2}+\frac{2\sin(\phi_R)y_Ry_I}{\zeta_R}}{\cos^2(\phi_R)[\sigma_n^2+\sigma_h^2|G_1x+G_2^*x^*+e|^2]}}}{\pi\zeta_R\cos(\phi_R)[\sigma_n^2+\sigma_h^2|G_1x+G_2^*x^*+e|^2]}. \tag{60}$$

Denote $Q = G_1x+G_2^*x^*+e$. Since e is a complex Gaussian random variable with $e \sim \mathcal{CN}(0,(\sigma_t^2+\sigma_r^2)P')$, Q is also a complex Gaussian random variable with $Q \sim \mathcal{CN}(G_1x+G_2^*x^*, (\sigma_t^2+\sigma_r^2)P')$. Hence, $|Q|$ is a Rician random variable and the unconditional PDF of y is

$$\begin{aligned} f(y) &= \int_0^\infty f(y|r)f_{|Q|}(r)dr = \frac{2e^{-\frac{|G_1x+G_2^*x^*|^2}{(\sigma_t^2+\sigma_r^2)P'}}}{\pi\zeta_R\cos(\phi_R)(\sigma_t^2+\sigma_r^2)P'} \\ &\quad \cdot \int_0^\infty \frac{rI_0(\frac{2r|G_1x+G_2^*x^*|}{(\sigma_t^2+\sigma_r^2)P'})}{\sigma_n^2+\sigma_h^2r^2} \\ &\quad e^{-\frac{y_R^2+\frac{y_I^2}{\zeta_R^2}+\frac{2\sin(\phi_R)y_Ry_I}{\zeta_R}}{\cos^2(\phi_R)}\frac{1}{\sigma_n^2+\sigma_h^2r^2}-\frac{r^2}{(\sigma_t^2+\sigma_r^2)P'}}dr, \end{aligned} \tag{61}$$

where the Rician PDF of $|Q|$ has been applied. This integral cannot be solved. However, when $\sigma_n^2 << \sigma_h^2$, one further has

$$\begin{aligned} f(y) &\approx \frac{2e^{-\frac{|G_1x+G_2^*x^*|^2}{(\sigma_t^2+\sigma_r^2)P'}}}{\pi\zeta_R\cos(\phi_R)(\sigma_t^2+\sigma_r^2)P'}\int_0^\infty \frac{I_0(\frac{2r|G_1x+G_2^*x^*|}{(\sigma_t^2+\sigma_r^2)P'})}{\sigma_h^2r} \\ &\quad e^{-\frac{y_R^2+\frac{y_I^2}{\zeta_R^2}+\frac{2\sin(\phi_R)y_Ry_I}{\zeta_R}}{\cos^2(\phi_R)}\frac{1}{\sigma_h^2r^2}-\frac{r^2}{(\sigma_t^2+\sigma_r^2)P'}}dr. \end{aligned} \tag{62}$$

A closed-form expression can be obtained by using the same method as (58) that expands the Bessel function into a series and solves the integral using [45, eq. (8.447.1)] and [45, eq. (3.478.4)] to give (24).

REFERENCES

[1] T. Schenk, *RF Imperfections in High-Rate Wireless Systems: Impact and Digital Compensation*, Springer, 2008.

[2] A.A. Boulogeorgos, V.M. Kapinas, R. Schober, G.K. Karagiannidis, "I/Q-imbalance self-interference coordination," *IEEE Trans. Wireless Commun.*, vol. 15, pp. 4157 - 4170 June 2016.

[3] T.C.W. Schenk, E. Fledderus, P.E.M Smulders, "Performance analysis of zero-IF MIMO OFDM transceivers with IQ imbalance," *Journal of Communications*, vol. 2, pp. 9 - 19, 2007.

[4] O. Ozdemir, R. Hamila, N. Al-Dhahir, "I/Q imbalance in multiple beamforming OFDM transceivers: SINR analysis and digital baseband compensation," *IEEE Trans. Commun.*, vol. 61, pp. 1914 - 1925, May 2013.

[5] J. Li, M. Matthaiou, T. Svensson, "I/Q imbalance in AF dual-hop relaying: performance analysis in Nakagami-m fading," *IEEE Trans. Commun.*, vol. 62, pp. 836 - 847, Mar. 2014.

[6] J. Li, M. Matthaiou, T. Svensson, "I/Q imbalance in two-way AF relaying," *IEEE Trans. Commun.*, vol. 62, pp. 2271 - 2285, July 2014.

[7] M. Mokhtar, A. Gomaa, N. Al-Dhahir, "OFDM AF relaying under I/Q imbalance: performance analysis and baseband compensation," *IEEE Trans. Commun.*, vol. 61, pp. 1304 - 1313, Apr. 2013.

[8] A.A. Boulogeorgos, P.C. Sofotasios, B. Selim, S. Muhaidat, G.K. Karagiannidis, M. Valkama, "Effects of RF impairments in communications over cascaded fading channels,"' *IEEE Trans. Veh. Technol.*, vol. 65, pp. 8878 - 8894, Nov. 2016.

[9] S. Javed, O. Amin, S.S. Ikki, M.-S. Alouini, "Asymmetric hardware distortions in receive diversity systems: outage performance analysis," *IEEE Access*, vol. 5, pp. 4491 - 4504, 2017.

[10] M. Matthaiou, A. Papadogiannis, E.Bjornson, M. Debbah, "Two-way relaying under the presence of relay transceiver hardware impairments," *IEEE Commun. Lett.*, vol. 17, pp. 1136 - 1139, June 2013.

[11] K. Guo, D. Guo, B . Zhang, "Performance analysis of two-way multi-antenna multi-relay networks with hardware impairments," *IEEE Access*, vol. 5, pp. 15971 - 15980, 2017.

[12] F. Ding, H. Wang, S. Zhang, M. Dai, "Impact of residual hardware impairments on non-orthogonal multiple access based amplify-and-forward relaying networks," *IEEE Access*, vol. 6, pp. 15117 - 15131, 2018.

[13] X. Xia, D. Zhang, K. Xu, W. Ma, Y. Xu, "Hardware impairments aware transceiver for full-duplex massive MIMO relaying," *IEEE Trans. Signal Processing*, vol. 63, pp. 6565 - 6580, Dec. 2015.

[14] E. Balti, M. Guizani, B. Hamdaoui, B. Khalfi, "Aggregate hardware impairments over mixed RF/FSO relaying systems with outdated CSI," *IEEE Trans. Commun.*, vol. 66, pp. 1110 - 1123, Mar. 2018.

[15] S. Cheng, R. Wang, J. Wu, W.. Zhang, Z. Fang, "Performance analysis and beamforming designs of MIMO AF relaying with hardware impairments," *IEEE Trans. Veh. Technol.*, vol. 67, pp. 6229 - 6243, July 2018.

[16] H. Wu, Y. Zou, W. Cao, Z. Chen, T.A. Tsiftsis, M.R. Bhatnagar, R.C. De Lamare, "Impact of hardware impairments on outage performance of hybrid satellite-terrestrial relay systems," *IEEE Access*, vol. 7, pp. 35103 - 35112, 2019.

[17] K. Guo, M. Lin, B. Zhang, W. Zhu, J. Wang, T.A. Tsiftsis, "On the performance of LMS communication with hardware impairments and interference," *IEEE Trans. Commun.*, vol. 67, pp. 1490 - 1505, Feb. 2019.

[18] K. Guo, K. An, B. Zhang, Y. Huang, D. Guo, G. Zheng, S. Chatzinotas, "On the performance of the uplink satellite multiterrestrial relay networks with hardware impairments and interference," *IEEE Systems J.*, vol. 13, pp. 2297 - 2308, Sept. 2019.

[19] E. Balti, M. Guizani, "Impact of non-linear high-power amplifiers on cooperative relaying systems," *IEEE Trans. Commun.*, vol. 65, pp. 4163 - 4175, Oct. 2017.

[20] E. Bjornson, M. Matthaiou, M. Debbah, "A new look at dual-hop relaying: performance limits with hardware impairments," *IEEE Trans. Commun.*, vol. 61, pp. 4512 - 4525, Nov. 2013.

[21] A.K. Mishra, D. Mallick, P. Singh, "Combined effect of RF impairment and CEE on the performance of dual-hop fixed-gain AF relaying,"' *IEEE Commun. Lett.*, vol. 20, pp. 1725 - 1728, Sept. 2016.

[22] A.K. Mishra, P. Singh, "Performance analysis of opportunistic transmission in downlink cellular DF relay network with channel estimation error and RF impairments," *IEEE Trans. Veh. Technol.*, vol. 67, pp. 9021 - 9026, Sept. 2018.

[23] M.M. Alsmadi, A.E. Canbilen, N. Abu Ali, S.S. Ikki, E. Basar, "Cognitive networks in the presence of I/Q imbalance and imperfect CSI: receiver design and performance analysis," *IEEE Access*, vol. 7, pp. 49765 - 49777, 2019.

[24] A.E. Canbilen, S.S. Ikki, E. Basar, S.S. Gultekin, I. Develi, "Joint impact of I/Q imbalance and imperfect CSI on SM-MIMO systems over generalized Beckmann fading channels: optimal detection and Cramer-Rao bound," *IEEE Trans. Wireless Commun.*, vol. 19, pp. 3034 - 3046, May 2020.

[25] B. Selim, S. Muhaidat, P.C. Sofotasios, B.S. Sharif, T. Stouraitis, G.K. Karagiannidi, N. Al-Dhahir, "Performance analysis of non-orthogonal multiple access under I/Q imbalance," *IEEE Access*, vol. 6, pp. 18453 - 18468, 2018.

[26] A.-A.A. Boulogeorgos, N.D. Chatzidiamantis and G.K. Karagiannidis, "Non-orthogonal multiple access in the presence of phase noise," *IEEE Communications Letters*, vol. 24, pp. 1133 - 1137, May 2020.

[27] A.-A. A. Boulogeorgos, N.D. Chatzidiamantis and G.K. Karagiannidis, "Energy detection spectrum sensing under RF imperfections," *IEEE Transactions on Communications*, vol. 64, pp. 2754 - 2766, July 2016.

[28] J. Sidrah, O. Amin, S.S. Ikki, M.-S. Alouini, "Asymmetric modulation for hardware impaired systems - error probability analysis and receiver design," *IEEE Trans. Wireless Commun.*, vol. 18, pp. 1723 - 1738, Mar. 2019.

[29] S. Javed, O. Amin, S.S. Ikki, M.-S. Alouini, "Multiple antenna systems with hardware impairments: new performance limits," *IEEE Transactions on Vehicular Technology*, vol. 68, pp. 1593 - 1606, 2019.

[30] Y. Gao, Y. Chen, N. Chen, J. Zhang, "Performance analysis of dual-hop relaying with I/Q imbalance and additive hardware impairment," *IEEE Trans. Veh. Technol.*, vol. 69, pp. 4580 - 4584, Apr. 2020.

[31] A.E. Canbilen, M.M. Alsmadi, E. Basar, S.S. Ikki, S.S. Gultekin, I. Develi, "Spatial modulation in the presence of I/Q imbalance: optimal detector & performance analysis," *IEEE Commun. Lett.*, vol. 22, pp. 1572 - 1575, Aug. 2018.

[32] A.E. Canbilen, S.S. Ikki, E. Basar, S.S. Gultekin, I. Develi, "Impact of I/Q imbalance on amplify-and-forward relaying: optimal detector design and error performance," *IEEE Trans. Commun.*, vol. 67, pp. 3154 - 3166, May 2019.

[33] T. Mao, Q. Wang, Z. Wang, "Receiver design for the low-cost teraHertz communication system with hardware impairment," *Proc. ICC 2020*, Dubin, Ireland, 7 - 11 June 2020.

[34] S. Bucher, G. Yammine, R.F.H. FIscher, C. Waldschmidt, "On the impact of hardware impairments in noncoherent massive MIMO systems," *Proc. 24th International ITG Workshop on Smart Antennas (WSA 2020)*, Hamburg, Germany, 2020.

[35] B. Selim, S. Muhaidat, P.C. Sofotasios, et al, "Performance analysis of coherent and noncoherent modulation under I/Q imbalance," *IEEE Access*, vol. 9, pp. 36125 - 36139, 2020.

[36] O.T. Demir, E. Bjornson, "Channel estimation in massive MIMO under hardware non-linearities: Bayesian methods versus deep learning," *IEEE Open J. of the Communi. Soc.*, vol. 1, pp. 109 - 124, 2020.

[37] O.T. Demir, E. Bjornson, "Channel estimation under hardware impairments: Bayesian methods versus deep learning," *Proc. ISWCS'19*, Oulu, Finland, Aug. 2019.

[38] Y. Wu, Y. Gu, and Z. Wang, "Efficient channel estimation for mmWave MIMO with transceiver hardware impairments," *IEEE Trans. Veh. Technol.*, vol. 68, pp. 9883 - 9895, Oct. 2019.

[39] Y. Wu, Y. Gu , and Z. Wang, "'Channel estimation for mmWave MIMO with transmitter hardware impairments," *IEEE Commun. Lett.*, vol. 22, pp. 320 -323, Feb. 2018.

[40] N. Kolomvakis, M. Matthaiou, M. Coldrey, "IQ imbalance in multiuser systems: channel estimation and compensation," *IEEE Trans. Commun.*, vol. 64, pp. 3039 - 3051, July 2016.

[41] N. Kolomvakis, M. Coldrey, T. Eriksson, and M. Viberg, "Massive MIMO systems with IQ imbalance: channel estimation and sum rate limits," *IEEE Trans. Commun.*, vol. 65, pp. 2382 - 2396, June 2017.

[42] B. Picinbono, "Second-order complex random vectors and normal distributions," *IEEE Trans. Signal Processing*, vol. 44, pp. 2637 - 2640, Oct. 1996.

[43] F.F. Digham, M.-S. Alouini and M.K. Simon, "On the energy detection of unknown signals over fading channels", *IEEE Trans. Commun.*, vol. 55, pp. 21-24, Jan. 2007.

[44] Y. Chen, "Improved energy detectors for random signals in Gaussian noise," *IEEE Trans. Wireless Commun.*, vol. 9, pp. 558 - 563, Feb. 2010.

[45] I.S. Gradshteyn, I.M. Ryzhik, *Tables of Integrals, Series and Products*, 6th Ed. Academic Press: London, 2000.

[46] J.G. Proakis, *Digital Communications*, 4th Ed. McGraw-Hill: New York, NY, 2000.

[47] M.Z. Win and R.A. Scholtz, "Impulse radio: how it works," *IEEE Commun. Lett.*, vol. 2, pp. 36-38, Feb. 1998.

[48] C. Carbonelli, U. Mengali, "M-PPM noncoherent receivers for UWB applications," *IEEE Trans. Wireless Commun.*, vol. 5, pp. 2285 - 2294, Aug. 2006.

[49] L. Tang, Y. Chen, E.L Hines, M.-S. Alouini, "Performance analysis of spectrum sensing with multiple status changes in primary user traffic," *IEEE Commun. Lett.*, vol. 16, pp. 874 - 877, June 2012.

[50] Q. Tao, C. Zhong, H. Lin, and Z. Zhang, "Symbol detection of ambient backscatter systems with Manchester coding," *IEEE Trans. Wireless Commun.*, vol. 17, pp. 4028 - 4038, June 2018.

[51] J.P.S. Sundaram, W. Du, Z. Zhao, "A survey on LoRa networking: research problems, current solutions, and open issues," *IEEE Commun. Sur. & Tut.*, vol. 22, pp. 371 - 388, First Quar. 2020.

[52] D.K.P. Tan, H. Sun, Y. Lu, M. Lesturgie, H.L. Chan, "Passive radar using Global System for Mobile communication signal: theory, implementation and measurements," *IEE Proceedings - Radar, Sonar and Navigation*, vol. 152, pp. 116 - 123, June 2005.

[53] J.M.F. Moura, Y. Jin, "Detection by time reversal: single antenna," *IEEE Trans. Signal Processing*, vol. 55, pp. 187 - 201, Jan. 2007.

[54] Y. Chen, N.C. Beaulieu, "Maximum likelihood estimation of SNR using digitally modulated signals," *IEEE Trans. Wireless Commun.*, vol. 6, pp. 210 - 219, Jan. 2007.

[55] S. Kay, *Fundamentals of Statistical Signal Processing: Estimation Theory*, Prentice Hall: New York, NY. 1993.